# Cellular, dendritic, and doublon patterns in directional crystallization

E. A. Brener

*Institute of Solid State Physics, Russian Academy of Sciences, 142432 Chernogolovka, Moscow Region, Russia*

D. E. Temkin

*Institute of Metal Science at I. P. Bardin Institute of Ferrous Metallurgy (State Research Center), 107005 Moscow, Russia*

This paper presents a generalization of the theory of the isothermal growth of cellular, dendritic, and doublon structures for directional crystallization under a temperature gradient. The theory takes into account the temperature gradient and the corresponding renormalization of thereby capillary effects, as well as the equations of mass balance in the diffusion problem. In the case of a cellular structure, the mass conservation equation relates the supercooling at the solidification front to the fraction of the solid phase in the cell. In dendritic and doublon structures, renormalization of the mass conservation equation corresponds to a modernization of the Ivantsov relation between supercooling and the Péclet number. The resulting equations relate supercooling at the solidification front to the crystallization rate. For all the types of solidification fronts, these functions are nonmonotonic and have minima. At growth rates much higher than the critical rate corresponding to the onset of the plane front instability, the functions coincide with those obtained in the case of the isothermal growth, when corrections due to the temperature gradient are small. We have found that the structure of the solidification front changes from cellular to dendritic and then to doublon as the growth rate increases. We present arguments that the first transition from cells to dendrites is gradual, i.e., the radius of curvature peaks of gradually drops as the growth rate increases, for a fixed period of the structure. The second transition, from dendrites to doublons, is sharp. like a first-order kinetic transition. © *1996 American Institute of Physics.* [S1063-7761(96)02703-1]

## 1. INTRODUCTION

In the process of controlled directional solidification, a thin sample of melt is drawn at a constant velocity $v$ across a region with a constant temperature gradient $G$. The propagating plane crystallization front becomes unstable over some wavelength range if the drawing velocity is larger than some critical velocity $v_c$ proportional to the temperature gradient and dependent on the melt composition. When the drawing velocity exceeds the critical value, a new stationary, periodic shape of the solidification front is established after some period of dynamic restructuring. Both the nonsteady growth and the final steady-state front shape are controlled by the ratio of velocities $v/v_c$.

The aim of our work was to describe analytically the basic types of growth front patterns and transitions between them. These structures include well-known cellular and dendritic structures,[1] and "doublon" structures recently discovered in experiments with directional crystal growth.[2,3] Our treatment of directional crystallization is based on the theory of growth of these structures under isothermal conditions. The corresponding papers include an investigation of growth of an isolated dendrite,[4] of a symmetric "finger" in a channel,[5–10] an asymmetric "finger" in a channel,[8–10] and of an isolated doublon.[10–12] The isolated doublon is a limiting case of an asymmetric finger in a channel close to one wall and far from the other.

In the case of isothermal growth, the problem is formulated as follows: determine the growth rate and typical dimensions of a grown structure at a given melt supercooling. In the case of directional crystallization, the growth rate is determined by the drawing rate, and the problem is to determine the supercooling at the solidification front (or the front position under a given temperature gradient) at a fixed growth rate. Since there is a temperature gradient, the equilibrium concentrations at the solid–liquid interface, which are functions of temperature determined by the equilibrium phase diagram, are also functions of the coordinates at the interface. This effect, which does not occur in isothermal growth, leads to a renormalization of both capillary effects and mass balance condition in the diffusion problem. As a result, the relation between supercooling and growth rate for different interface structures in directional solidification is very different from that in the case of isothermal growth.

The paper is organized as follows. Section 2 contains basic equations describing the directional crystallization of a binary alloy under a linear temperature gradient. Section 3 describes capillary length renormalization due to the temperature gradient. Sections 4, 5, and 6 describe the cellular, dendritic, and doublon patterns, respectively. In Section 7 we discuss the results and propose the following sequence of growth patterns versus the growth rate: cells, dendrites, doublons.

1063-7761/96/030559-08$10.00

## 2. STATEMENT OF THE PROBLEM; BASIC EQUATIONS

In this paper we consider crystallization of a binary dilute alloy under a temperature gradient $G$. Diffusion is taken into account only in the liquid phase. The concentration field $C(x,z)$ in the melt and the crystallization front shape $\zeta(x)$ in the steady-state two-dimensional process are described by

$$\nabla^2 C + \frac{v}{D}\frac{\partial C}{\partial z} = 0 \tag{1}$$

(the initial concentration in the melt far ahead of the growth front is $C_\infty$). The mass balance equation at the solidification front is

$$-D\frac{\partial C}{\partial n} = C_i(1-k)v\cos\Theta, \tag{2}$$

where $v$ is the drawing velocity, $D$ is the diffusion coefficient in the melt, $k$ is the impurity distribution coefficient, and $\Theta$ is the angle between the normal to the interface and the growth axis $Oz$ aligned with the temperature gradient. The concentration in the melt near the interface is assumed to be equilibrium and determined by the Gibbs–Thomson condition:

$$C_i = \frac{C_\infty}{k} - \frac{Gz}{m} - \frac{\bar{\gamma}(\Theta)T_m}{Lm}K. \tag{3}$$

The origin, $z=0$, corresponds to the solidus temperature $T_S$ of the initial melt composition $C_\infty$, $T_S = T_m - mC_\infty/k$, $T_m$ is the melting temperature of the pure material, $m/k = -\partial T_S/\partial C$ determines the slope of the solidus line, $L$ is the latent heat of fusion, $\bar{\gamma}(\Theta) = \gamma(\Theta) + \gamma''(\Theta)$, where $\gamma(\Theta)$ is the surface energy of the interface, which is assumed to be anisotropic in the general case, and $K = -\zeta''/(1+\zeta'^2)^{3/2}$ is the curvature of the crystallization front.

Although the problem seems fairly simple, its solutions describe various shapes of the solidification front, namely, shallow and deep periodic cells, dendrites and doublons, various random structures, etc. One formulation of the problem is to determine the shape and location of the crystallization front for a given temperature distribution at a fixed wavelength of the grown structure. The more profound problem of the wavelength selection of the grown structure has been discussed extensively in the literature, but its ultimate solution has not been found yet (see Ref. 13 and references therein).

In this paper we discuss three types of structures: periodic cellular, dendritic, and doublon (Fig. 1). The theory of their growth has been developed for the case of isothermal crystallization ($G=0$). There are publications on the growth of an isolated dendrite,[4] crystal growth in a channel,[5–10] and doublon growth.[8–12] An important feature of these theories is that they take into account the interface curvature in Eq. (3) as a singular perturbation to the equation for the growth front shape. These theories yield solvability conditions for equations of the growth front shape in the form of selection relations. For example, in the case of an isolated dendrite at zero temperature gradient, the selection relation has the form[4]
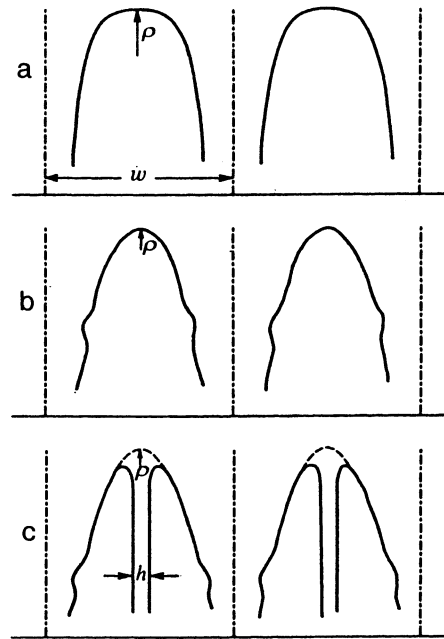


FIG. 1. Three patterns of two-dimensional crystallization fronts: a) cellular structure; b) dendritic structure; c) doublon structure; $\rho$ is the radius of curvature at the peak (in the doublon pattern $\rho$ is the radius of curvature of the envelope); $w$ is the structure period.

$$\frac{2d_0 D}{v\rho^2 C_0(1-k)} = \sigma^*(\alpha), \tag{4}$$

where $d_0 = \bar{\gamma}_0 T_m/Lm$ is the capillary length, $\rho$ is the radius of curvature of the dendrite peak, $C_0$ is the equilibrium solute concentration in the melt at a given temperature, $\sigma^*(\alpha)$ is a known function of the surface energy anisotropy parameter, $\alpha$. In the case of four-fold anisotropy $[\bar{\gamma}(\Theta) = \bar{\gamma}_0(1 - \alpha \cos 4\Theta)]$ and at a small $\alpha$, the function is $\sigma^*(\alpha) \sim \alpha^{7/4}$. One effect of the temperature gradient is a change in selection relations like Eq. (4). This change may be formalized as a renormalization of the capillary length $d_0$.

## 3. RENORMALIZATION OF THE CAPILLARY LENGTH DUE TO A TEMPERATURE GRADIENT

The renormalization procedure was described in Refs. 14 and 15 and is performed as follows. A new field $\tilde{C}$ is introduced so that Eqs. (2) and (3) have the same form as the equations for the isothermal problem, i.e., Eq. (3) must contain no $z$-dependent terms. It is known[4] that in the isothermal case the selection relation (4) can be derived by replacing Eq. (1) with the Laplace equation at a sufficiently small velocity $v$:

$$\nabla^2 C = 0, \tag{5}$$

and by replacing the concentration $C_i$ in Eq. (2) by $C_0$:

$$-D\frac{\partial C}{\partial n} = C_0(1-k)v\cos\Theta. \tag{6}$$

In the isothermal case Eq. (3) is transformed to

$$C_i = C_0 - d_0(\Theta)K. \tag{7}$$

In solving the problem of directional crystallization under a temperature gradient, we also replace in Eq. (2) the local concentration $C_i$ determined by Eq. (3) with the constant $C_0$, which equals the equilibrium concentration at the temperature of the peak (the omission of the term depending on the curvature is justified by the same arguments as in the isothermal approximation). The dependence of $C_i$ on the coordinate $z$ may be ignored because in the derivation of the selection relations the only essential variations are those over a length comparable to $\rho$, which are small at a fairly small gradient $G$:

$$\frac{\rho G}{m C_\infty(1/k - 1)} \ll 1.$$

Thus we can derive the selection relations from Eqs. (5) and (6) and the unchanged Eq. (3). Introducing the new concentration field $\widetilde{C}$ instead of $C$ using relation

$$C = \frac{C_\infty}{k} - \frac{Gz}{m} + \left[1 - \frac{DG}{vmC_0(1-k)}\right](\widetilde{C} - C_0), \tag{8}$$

we obtain the same Eqs. (5)–(7) for $\widetilde{C}$ with $C$ replaced by $\widetilde{C}$ and $d_0(\Theta)$ by $\widetilde{d}_0(\Theta)$:

$$\widetilde{d}_0(\Theta) = d_0(\Theta)\left[1 - \frac{DG}{vmC_0(1-k)}\right]^{-1}. \tag{9}$$

Using this renormalization of the capillary length, we can write instead of Eq. (4) a selection relation for an isolated dendrite under a temperature gradient:

$$\frac{2d_0 D}{v\rho^2 C_0(1-k)}\left[1 - \frac{DG}{vmC_0(1-k)}\right]^{-1} = \sigma^*(\alpha). \tag{10}$$

## 4. CELLULAR PERIODIC STRUCTURE

Our aim is to find the temperature on a cellular structure growth front as a function of the period $w$ and the growth velocity $v$. This problem was analyzed by many researchers[14–16] using its similarity to the Saffman–Taylor problem at small Péclet numbers. But the analysis of crystallization of a pure substance in a channel[7–10] demonstrated that the difference between the crystallization problem, which is described by the diffusion equation, and the Saffman–Taylor problem, which reduces to the Laplace equation, is significant, even at small Péclet numbers. Using the solution for the isothermal growth of a pure substance and the renormalization of the capillary length given by Eq. (9), we shall write the selection relations for the isothermal growth of an alloy in a channel of width $w$ at a supercooling

$$\Delta = \frac{C_0 - C_\infty}{C_0(1-k)}, \tag{11}$$

where $C_0$ is the equilibrium concentration in the melt at a given temperature $T_0$. From Eqs. (4.4) and (4.13) in Ref. 7 we derive

$$\frac{d_0 D}{vw^2 C_0(1-k)} = \frac{1}{8\mu}\frac{[1 - \pi^2/(\lambda s)^2]^{3/2}}{s^2}, \tag{12}$$

where $\mu \simeq 1/3$ is a numerical factor and

$$s = -\frac{vw}{2D} + \sqrt{\left(\frac{vw}{2D}\right)^2 + \left(\frac{\pi}{1-\lambda}\right)^2}. \tag{13}$$

The parameters $s$ and $\lambda$ determine the shape of the crystallization front, which is assumed to have the Saffman–Taylor form,

$$\zeta = z_0 + \frac{w}{s}\ln\cos\frac{\pi x}{\lambda w}, \tag{14}$$

where $z_0$ is the location of the peak. The relative width $\lambda$ of the rod is determined by mass balance, and in isothermal crystallization

$$\lambda = \Delta. \tag{15}$$

In crystallization directional crystallization at a given temperature gradient, Eqs. (11)–(15) are modified in the following way. If the temperature gradient is fairly small so that

$$wGk/[mC_\infty(1-k)] \ll 1,$$

the front shape over a distance $w$ is the same as in isothermal crystallization, and is described by Eqs. (13) and (14). Subsequent complete crystallization takes place over a length

$$(z - z_0) \sim l_T = mC_\infty(1-k)/Gk \gg w.$$

Given that the temperature gradient is small, we define $C_0$ in Eq. (11) as the equilibrium concentration at temperature $T_0$ at the peak of the structure, and $\Delta$ in Eq. (11) is the super-cooling at the peak. In Eq. (12) the renormalized capillary length $\widetilde{d}_0$ defined by Eq. (9) must be used instead of $d_0$. (In this section we ignore capillary length anisotropy in the analysis of cellular structure.) Taking account of the temperature gradient in the mass conservation condition, Eq. (15) is modified[15]:

$$\Delta = \left[\lambda + (1-\lambda)\frac{v_c}{vk}\right]\left[1 + (1-\lambda)\frac{v_c(1-k)}{vk}\right]^{-1}, \tag{16}$$

where $v_c$ is the critical growth velocity corresponding to the onset of instability at a plane front, capillary effects being ignored:

$$v_c = GDk/mC_\infty(1-k). \tag{17}$$

Equation (16) can be easily derived from the effective conservation equation for diffusion near the peak of the structure at $z \simeq z_0$:

$$-D\frac{\partial C}{\partial z}\bigg|_{z_0+0} = v\lambda C_0(1-k) - (1-\lambda)D\frac{\partial C}{\partial z}\bigg|_{z_0-0}. \tag{18}$$

Assuming that diffusion fields can be described by one-dimensional functions both ahead of the peak,

$$C(z) = C_\infty + (C_0 - C_\infty)\exp\left[-\frac{v(z-z_0)}{D}\right], \quad z > z_0,$$

and behind it,

$$C(z) = C_\infty/k - Gz/m, \quad z < z_0,$$

we derive Eq. (16) from Eq. (18).

Let us introduce dimensionless parameters

$$V = \frac{v d_0}{2D C_\infty (1-k)}, \quad V_c = \frac{v_c d_0}{2D C_\infty (1-k)},$$

$$W = \frac{w C_\infty (1-k)}{d_0} \qquad (19)$$

and transform Eqs. (12), (13), and (16) by replacing $d_0$ with the renormalized length $\tilde{d}_0$ defined by Eq. (9):

$$s = -VW + \sqrt{(VW)^2 + \left(\frac{\pi}{1-\lambda}\right)^2}, \qquad (20)$$

$$\frac{1-\lambda(1-k)}{2VW^2(1-V_c/V)} = \frac{1}{8\mu} \frac{[1-\pi^2/(\lambda s)^2]^{3/2}}{s^2}, \qquad (21)$$

$$\Delta = \left[\lambda + (1-\lambda)\frac{V_c}{Vk}\right]\left[1 + (1-\lambda)\frac{V_c(1-k)}{Vk}\right]^{-1}. \qquad (22)$$

These equations determine the shape parameters, $s$ and $\lambda$, and the supercooling $\Delta$ at the peak as functions of the growth velocity $V$ and structure period $W$. The real difference between our analysis and that in Ref. 15 is that the Péclet number is included in Eq. (20). As a result, the supercooling $\Delta$ at the peak is a nonmonotonic function of the period. If we adopt the hypothesis that the operating point of the growth process is at the minimum of the supercooling $\Delta$ as a function of the period $W$, these two parameters can be determined as functions of the pulling velocity $V$. Our analysis indicates that in the range of realistic parameters $\lambda$ is close to 1/2 (the supercooling may significantly differ from 1/2). Given that $\lambda - 1/2$ and the Péclet number $VW$ are small, we derive from Eqs. (20) and (21)

$$(\lambda - 1/2) \simeq \frac{VW}{8\pi} + \frac{1}{4}\left[\frac{4\mu\pi^2(1+k)}{\sqrt{2}VW^2(1-V_c/V)}\right]^{2/3}. \qquad (23)$$

It follows from Eq. (22) that $\partial\Delta/\partial\lambda > 0$. Therefore the extremum of $\Delta(W)$ coincides with that of $\lambda(W)$. At the extremum $d\lambda/dW = 0$, hence

$$W_m \simeq \pi\left[\frac{64\mu(1+k)}{3\sqrt{3}V^{5/2}(1-V_c/V)}\right]^{2/7}, \qquad (24)$$

$$\lambda_m - \frac{1}{2} \simeq \frac{7}{8}\left[\frac{\mu(1+k)V}{6\sqrt{3}(1-V_c/V)}\right]^{2/7}, \qquad (25)$$

and $\Delta$ is determined by Eq. (22) at $\lambda = \lambda_m$. These equations are valid if $\lambda - 1/2 \ll 1$. They do not hold in a narrow range of velocities around the critical velocity $V_c$,

$$(V - V_c)/V_c < V_c \ll 1, \qquad (26)$$

and at very large velocities,

$$V > 1 \gg V_c.$$

Since typical values are $V_c \sim 10^{-5} - 10^{-4}$, the range where Eqs. (23)–(25) are valid is fairly wide. The resulting function of $\Delta$ versus $V$ is nonmonotonic (Fig. 2). In the two limiting cases, $V \to V_c$ and $V \to \infty$, the supercooling $\Delta$, as well as $\lambda_m$, tends to unity. As was noted above, these two limiting cases are not described by Eq. (25) and formally can be analyzed using more general equations (20)–(22) at $\lambda \to 1$.
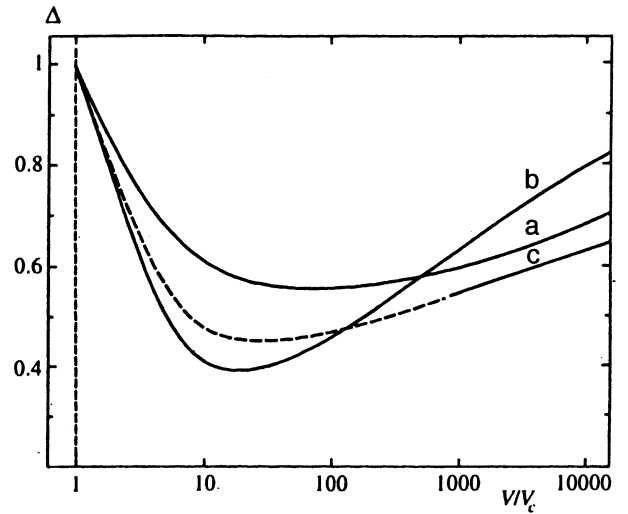


FIG. 2. Dimensionless supercooling, $\Delta$, at the peak versus reduced growth velocity: a) a curve for cellular structure calculated using Eqs. (22) and (25); b) a curve for dendritic structure calculated using Eq. (38); c) a curve for doublon structure calculated using Eq. (50). The calculations used the following parameters: $V_c = 10^{-5}$, $k = 1/3$, $\sigma^* = 0.02$. The entire curve c, including the dashed portion, corresponds to the isotropic case, $\alpha = 0$. The solid portion of curve c shows the domain of the doublon solution defined by the criterion of Eq. (47) with an anisotropy parameter $\alpha = 0.1$ (see details in the text).

Note, however, that the selection relation (21) was derived at $\lambda$ close to 1/2. Nonetheless, the nonmonotonic function $\Delta(V)$ is described by Eqs. (22) and (25) over a wide range of parameters. The supercooling is minimum, $\Delta_m$, at a growth velocity

$$V/V_c \simeq \left[\frac{6\sqrt{3}}{\mu(1+k)V_c}\right]^{2/9}\left(\frac{1+k}{k}\right)^{7/9}. \qquad (27)$$

Since $V_c \ll 1$, the point of extremum is at $V/V_c \gg 1$. At this velocity the minimum supercooling is

$$\Delta_m \simeq \frac{1}{2} + \frac{1}{4}\left[\frac{\mu(1+k)^2 V_c}{6\sqrt{3}k}\right]^{2/9}. \qquad (28)$$

## 5. DENDRITIC GROWTH IN DIRECTIONAL CRYSTALLIZATION

In addition to cellular structures, dendrites are clearly seen at the crystallization front in some experiments on directional growth. The basic difference between the cellular and dendritic structures is that the peak radius $\rho$ of a dendrite is much smaller than the structure period $w$ (separation between neighboring dendrites), whereas in cellular structures these two parameters are comparable. In this section we describe dendritic structure. As a first step, let us consider the growth of an isolated dendrite at $w \to \infty$. Here we do not consider the interaction between dendrites, which determines, in the long run, the separation between them.[13]

It is known that the isothermal growth of an isolated dendrite is described by two equations. The first relates the Péclet number $p = v\rho/2D$ of the grown dendrite to the supercooling $\Delta$, capillary effects at the interface being ignored[17]:

$$\Delta = \sqrt{\pi p} \, \exp(p) \, \mathrm{erfc}(\sqrt{p}). \tag{29}$$

This equation was derived for the case of two-dimensional crystallization; here $\Delta$ is determined by Eq. (11). The second equation is the selection relation (4). These two equations determine the growth velocity $v$ and the peak radius $\rho$ as functions of the supercooling $\Delta$. In directional crystallization under a temperature gradient, the dendrite growth rate is determined by that of pulling. The problem is to derive the peak radius $\rho$ and the supercooling $\Delta$ at the dendrite peak from given growth parameters, namely the velocity $v$ and temperature gradient $G$. To this end, we use Eq. (10) with the capillary length renormalized taking into account the temperature gradient instead of Eq. (4). The Ivantsov relation (29) must be also modified to include the temperature gradient. Our modification is based on the boundary-layer model (BLM), which yields an approximate but qualitatively correct relation between the Péclet number $p$ and the supercooling $\Delta$ in the case of isothermal growth[18]:

$$p = \Delta^2/2(1-\Delta)$$

(compare to the exact equation (29)). The BLM steady-state equation for alloy crystallization, which replaces Eqs. (1) and (2), has the form[19]

$$\frac{k^2 v}{KD}(1-U)\cos\Theta - \frac{U^2}{[1+U(1/k-1)]\cos^2\Theta}$$

$$- \tan\Theta \frac{d}{d\Theta}\left[\frac{U^2}{1+U(1/k-1)}\right]$$

$$+ \frac{D}{v}\frac{d}{d\Theta}\left[\frac{KU}{[1+U(1/k-1)]\cos\Theta}\frac{dU}{d\Theta}\right] = 0, \tag{30}$$

where

$$U = (C_i - C_\infty)/C_\infty(1/k-1)$$

is the dimensionless solute concentration in the melt at the growth surface, which is determined, according to Eq. (3), by the equation

$$U = 1 - \frac{Gk}{mC_\infty(1-k)}z - \frac{d_0 k}{C_\infty(1-k)}K. \tag{31}$$

Recall that $\Theta$ is the angle between the growth axis $z$ and the normal to the solidification front. In order to derive the equation relating the Péclet number to the supercooling, we omit the term due to the capillary effect in Eq. (31). By differentiating Eq. (31) with respect to $\Theta$, we obtain

$$\frac{dU}{d\Theta} = \frac{v_c \sin\Theta}{DK(\Theta)}, \tag{32}$$

where the critical velocity $v_c$ is determined by Eq. (17). By expanding in powers of $\Theta$ the unknown functions $U(\Theta)$ and $K(\Theta)$ around $\Theta = 0$,

$$U(\Theta) = U_0 + \frac{v_c \Theta^2}{2DK_0} + \ldots,$$

$$K(\Theta) = K_0 + a\Theta^2 + \ldots, \tag{33}$$

we derive from Eq. (30) near the dendrite peak at $\Theta \to 0$

$$K_0 = \frac{k^2 v}{D}\frac{(1-U_0)[1+U_0(1/k-1)]}{U_0^2(1-v_c/vU_0)}. \tag{34}$$

Given the relationship between $U_0$ and the supercooling $\Delta$ at the dendrite peak,

$$U_0 = \frac{C_0 - C_\infty}{C_\infty(1/k-1)} = \frac{k\Delta}{1-(1-k)\Delta}, \tag{35}$$

we derive from Eq. (34)

$$p = \frac{v\rho}{2D} = \frac{\Delta^2}{2(1-\Delta)}\left[1 - \frac{v_c}{v}\frac{[1-(1-k)\Delta]}{k\Delta}\right]. \tag{36}$$

Here the peak radius $\rho = 1/K_0$, and the supercooling $\Delta$ at the dendrite peak is determined by Eq. (11). Equation (36) replaces the Ivantsov relation (29). We rewrite the selection condition (10) as

$$\frac{2d_0 D}{v\rho^2 C_\infty(1-k)}\frac{1-(1-k)\Delta}{\left[1-\dfrac{v_c[1-(1-k)\Delta]}{vk}\right]} = \sigma^*. \tag{37}$$

The parameter $\rho$ is eliminated from Eqs. (36) and (37), and dimensionless velocities $V$ and $V_c$ are introduced, according to Eq. (19). Hence follows the final equation relating the supercooling $\Delta$ at the dendrite peak to the growth velocity $V$:

$$\frac{V}{\sigma^*}\frac{[1-(1-k)\Delta]}{\left[1-\dfrac{V_c[1-(1-k)\Delta]}{Vk}\right]}$$

$$= \frac{\Delta^4}{4(1-\Delta)^2}\left[1 - \frac{V_c}{V}\frac{[1-(1-k)\Delta]}{k\Delta}\right]^2. \tag{38}$$

As in the case of cellular structure, $\Delta(V)$ has a minimum (Fig. 2). At $V \to V_c$ the supercooling, $\Delta$ tends to unity:

$$(1-\Delta) \simeq \left(\frac{\sigma^*}{4kV_c}\right)^{1/2}\left(1 - \frac{V_c}{V}\right)^{3/2}. \tag{39}$$

We stress that Eq. (39) is most probably inaccurate, because at $V \to V_c$ the Péclet number diverges as $(1-V/V_c)^{-1/2}$, as follows from Eqs. (36) and (39), whereas the selection equation (37) and the capillary length renormalization were derived at moderate Péclet numbers. If $V_c$ is small, there is an intermediate asymptote as $V \to V_c$, namely, at

$$\frac{V_c k^3}{\sigma^*} \ll \left(\frac{V}{V_c}\right) - 1 \ll 1$$

we have

$$(1-\Delta) \simeq k(V/V_c - 1). \tag{40}$$

As $(V)$ increases, $\Delta(V)$ goes through a minimum. The minimum supercooling $\Delta_m$ is described by the equation

$$\frac{\Delta_m^5}{(1-\Delta_m)^2}\frac{(b-2\Delta_m)(b-2)^2}{[1-(1-k)\Delta_m]^2 b^4} = \frac{2V_c}{k\sigma^*}, \tag{41}$$

where $b$ is a function of $\Delta_m$:

$$b(\Delta_m) = 3 + 2\Delta_m + \sqrt{8 + (1-2\Delta_m)^2},$$

and the velocity at the minimum depends on $\Delta_m$:

$$V_m/V_c = b(\Delta_m)[1 - (1-k)\Delta_m]/2k\Delta_m. \qquad (42)$$

At the parameters of Fig. 2, the minimum has the coordinates $V_m/V_c \simeq 18.7$, $\Delta_m \simeq 0.392$. At larger velocities $(V \gg V_c)$, we have the same relation between $\Delta$ and $V$ as in dendritic growth under isothermal conditions:

$$V \simeq \frac{\sigma^*}{1 - (1-k)\Delta} \frac{\Delta^4}{4(1-\Delta)^2}. \qquad (43)$$

Note that formally Eq. (38) has two additional solutions $\Delta(V)$ at $V \sim V_c$. These solutions define a closed loop in the $\Delta$–$V$ plane. But these solutions are unphysical, since the Péclet number [Eq. (36)] for them is negative.

## 6. DOUBLON GROWTH IN DIRECTIONAL CRYSTALLIZATION

In crystal growth, the doublon structure[2,3,10] may compete with both cellular and dendritic structures. In this section we modify the theory of isolated doublon growth[12] similarly to the previous section. Doublon growth under isothermal conditions is described in the following way. Doublon shape is defined by two parameters: the radius of curvature $\rho$ of the envelope parabola at the peak and the width $h$ of the liquid layer far from the peak (Fig. 1). The Péclet number $p = v\rho/2D$ for the envelope parabola is related to the supercooling $\Delta$ by the Ivantsov relation (29). The dimensions $h$ and $\rho$ are interdependent, and their relation at small Péclet numbers is described by the equation[12]

$$h/\rho \simeq \pi/4. \qquad (44)$$

Finally, there is a selection relation between the parameter

$$\sigma = \frac{2d_0 D}{v\rho^2 C_0(1-k)}, \qquad (45)$$

and the Péclet number[12]:

$$\sigma \sim (ph/\rho)^{5/2}. \qquad (46)$$

Equations (44) and (46) describe doublon growth in an isotropic system: the anisotropy parameter $\alpha$ is zero. In anisotropic systems with a small but finite parameter $\alpha$, steady doublon growth is not possible at all supercoolings, but only when the Péclet number $p(\Delta)$ is larger than a critical value, which is a function of the anisotropy parameter $\alpha$:

$$p(\Delta) > \alpha^{1/2}. \qquad (47)$$

This condition was derived for four-fold symmetry.[12] In the domain of the doublon solution, i.e., when the condition (47) is met, the selection is approximately determined by the same equations (44) and (46), which contains only expansion terms of the zeroth order in $\alpha$. We propose a modification procedure for directional crystallization under a temperature gradient similar to the case of dendrite growth (Section 5):

a) the relationship between the Péclet number $p$ for the envelope parabola and the supercooling $\Delta$ near the peak is determined by Eq. (36):

$$p = \frac{v\rho}{2D} = \frac{\Delta^2}{2(1-\Delta)}\left[1 - \frac{v_c}{v}\frac{1-(1-k)\Delta}{k\Delta}\right]; \qquad (48)$$

b) the capillary length $d_0$ in the definition of $\sigma$ (Eq. (45)) is replaced by the renormalized length defined by Eq. (9):

$$\sigma = \frac{2d_0 D}{v\rho^2 C_\infty(1-k)}\frac{1 - (1-k)\Delta}{1 - \dfrac{v_c[1 - (1-k)\Delta]}{vk}}. \qquad (49)$$

Note that the gap $h$ in the middle of the doublon is closed at a distance of the order of the thermal length $l_T$, which is expected to be much larger than the radius $\rho$.

After eliminating the parameter $\rho$ from Eqs. (44), (46), (48), and (49) and introducing the dimensionless velocities $V$ and $V_c$ (Eq. (19)), we obtain the equation relating the supercooling $\Delta$ at the peak to the growth velocity $V$:

$$V\frac{1 - (1-k)\Delta}{1 - \dfrac{V_c[1 - (1-k)\Delta]}{Vk}} \approx \left[\frac{\Delta^2}{2(1-\Delta)}\left(1 - \frac{V_c}{V}\frac{[1 - (1-k)\Delta]}{k\Delta}\right)\right]^{9/2}. \qquad (50)$$

The resulting relation between $\Delta$ and $V$ for a doublon grown in an isotropic system has a minimum, given by Eq. (50), like those of the cellular and dendritic structures (Fig. 4, curve c). At $V \gg V_c$, the same relation as for the isothermal doublon growth can be obtained:

$$V \approx \frac{1}{1 - (1-k)\Delta}\left[\frac{\Delta^2}{2(1-\Delta)}\right]^{9/2}. \qquad (51)$$

At $V$ close to $V_c$ the supercooling is approximately equal to unity:

$$(1-\Delta) \approx \frac{1}{2}\left(\frac{1}{kV_c}\right)^{2/9}\left(1 - \frac{V_c}{V}\right)^{11/9}. \qquad (52)$$

Note that, as in the case of dendrite growth (Section 5), Eq. (52) does not hold at $V \to V_c$ since the Péclet number increaseses without bound as $(1 - V/V_c)^{-2/9}$, whereas the theory was developed for small Péclet numbers. In the case of anisotropy, Eqs. (50)–(52) are valid only in the domain of the doublon solution, i.e., when the additional condition (47) holds. As a result, a solution exists in only two ranges of the growth velocity: near $V_c$, when $V_c < V < V_1$, and beyond another critical velocity, $V > V_2$, so no solution exists in the intermediate range $V_1 < V < V_2$. If $\alpha$ is relatively large, the critical velocities $V_1$ and $V_2$ may be estimated using the asymptotic relations in Eqs. (51) and (52), and Eqs. (47) and (48):

$$(V_1 - V_c)/V_c \sim kV_c\alpha^{-9/4}, \qquad (53)$$

$$V_2/V_c \sim \alpha^{9/4}/V_c. \qquad (54)$$

In this derivation we assume that $V_c/\alpha^{9/4}$ is small. Otherwise, when this parameter is large, we obtain $V_1 > V_2$, i.e., the doublon solution exists throughout the whole velocity range $V > V_c$. A situation in which the solution exists at all velocities is possible when $\alpha$ is smaller than some critical value, $\alpha < \alpha_c$, which can be estimated by taking $V_1 \sim V_c$. This estimate yields $\alpha_c \sim V_c^{4/9}$. At parameters given in Fig. 1 the solid portion of curve c corresponds to velocities $V > V_2$. The parameter $V_1$ is very close to $V_c$, and they cannot be distinguished in Fig. 2.

# 7. DISCUSSION

We have discussed three types of growth morphologies in directional crystallization: cellular, dendritic, and doublon (Fig. 1). Supercooling is plotted as a function of growth velocity in Fig. 2. The basic difference between cellular structure and the other two types is that its peak radius is comparable to the structure period, whereas in dendritic and doublon structures the peak radius is much smaller than the structure period. In fact we ignored the diffusion interaction between different stems of the dendritic and doublon structures assuming that the structure period was larger than the diffusion length, $D/v$. The curves of the supercooling versus the solidification velocity are nonmonotonic in all three cases (Fig. 2). All these curves originate from the point $V/V_c = 1$, $\Delta = 1$, corresponding to the onset of the plane solidification front instability. Near the critical point, the supercooling drops with increasing growth velocity, and after passing the minimum increases. At $V \gg V_c$ the rising portions of the curves are, naturally, described by the equations for isothermal growth. Under these conditions, the effect of the temperature gradient is small.

In the case of cellular structure, the period and the curvature radius are comparable, and supercooling at the front is a function not only of $V/V_c$, but also of the structure period. The solution of the Laplace equation for this structure[15] instead of the diffusion equation yields the monotonically decreasing function $\Delta(w)$, with $w$ entering in the form of a dimensionless parameter $w^2 v/d_0 D$. Analysis in the context of the diffusion equation (i.e., at a finite Péclet number, $vw/D$) yields a minimum in $\Delta(w)$. Curve a in Fig. 2 shows $\Delta$ as a function of $V/V_c$ for cellular structure, which corresponds to the function $\Delta(v,w)$ being minimized with respect to the period $w$. In other words, the curve is plotted not for an arbitrary period, but for the period corresponding to minimum supercooling. At a different period $w$, the curve of $\Delta(V/V_c)$ would be similar, but higher than curve a in Fig. 2. In fact, we have selected the cellular structure period by minimizing the supercooling, although we must stress that there is no deep underlying physical reason for this selection. The period of the cellular structure determined by the minimization versus the growth velocity is given by Eq. (24). At $V/V_c \gg 1$ the period drops with velocity as

$$W_m \simeq 5(1+k)^{2/7} V^{-5/7}.$$

If we use this hypothesis of the minimum supercooling to select the structure, one can see in Fig. 2 that dendritic structure is preferable at moderate growth velocities, and it seems that the domain of cellular structure vanishes. But experimental data clearly indicate that the cellular structure is grown at a velocity several times higher than $V_c$, and the transition to dendritic structure takes place at $V/V_c \sim 10$. In our opinion, the fact that cellular structure is produced at a growth velocity close to $V_c$ can be explained as follows. In order to produce dendritic structure, the period must be at least larger than $2\rho$, where $\rho$ is the dendrite peak radius. The structure period due to plane front instability is of the order of the Mullins–Sekerka length at a velocity of order $v_c$:

$$w \simeq 2\pi \sqrt{\frac{d_0 k D}{C_\infty(1-k)v_c}}.$$

Increases in the structure period take place extremely inefficiently. By estimating the peak radius $\rho$ from Eq. (37) and taking $2\rho/w \sim 1$, we find that dendritic structure should appear at $V/V_c > 1/(\pi^2 \sigma^* k)$. At the parameters selected in our study, $\sigma^* = 0.02$ and $k = 1/3$, we have $V/V_c > 15$, and cellular structure should occur at lower velocities. Note that the transition from cells to dendrites is gradual. In fact, at a fixed structure period, the peak radius decreases with growth velocity, and at $\rho/w \ll 1$ dendritic structure is clearly seen and has well-developed side branches. The selection of the period of well-developed dendritic structure was studied by Warren and Langer,[13] and they demonstrated that the pattern selection is history-dependent, namely, it is determined by the transition from the plane solidification front through instability to developed dendritic structure.

The doublon solution at parameters selected in this study (including the case of the anisotropy parameter $\alpha = 0.1$) exists only at $V/V_c > 10^3$ and is more preferable in this range since it has the lowest supercooling at a given velocity.

Our analysis indicates that the shape of the solidification front changes with velocity in the following sequence: cells, dendrites, then doublons. The transition from cells to dendrites was detected long ago, and the second transition from dendrites to doublons was discovered quite recently.[2,3] In our opinion, unlike the gradual cell–dendrite transition, the dendrite–doublon transition is sharp, like a first-order kinetic transition, and leads to a jump in the supercooling at the front. Note that a similar transition from dendritic to "seaweed" structure was described in Ref. 20. Subsequent studies of the isothermal growth of asymmetric structures[8–10,14] demonstrated that the doublon is a basic component of "seaweed" structure.

[1] W. Kurz and D. J. Fisher, *Fundamentals of Solidification*, Trans. Tech., Switzerland (1984); H. Müller-Krumbhaar and W. Kurz, *Phase Transformation in Materials*, P. Haasen (e.d.), VCH-Verlag, Weinheim (1991).

[2] H. Jamgotchian, R. Trivedi, and B. Billia, Phys. Rev. E **47**, 4313 (1993).

[3] S. Akamatsu, G. Faivre, and T. Ihle, Phys. Rev. E **51**, 4751 (1995).

[4] J. S. Langer, in *Chance and Matter*, Les Houches Lectures XLVI, Elsevier, New York (1987); D. Kessler, J. Koplik, and H. Levine, Adv. Phys. **37**, 255 (1988); E. A. Brener and V. I. Melnikov, Adv. Phys. **40**, 53 (1991); Y. Pomeau and M. Ben Amar, in *Solids Far From Equilibrium*, C. Godréche (ed.), Cambridge University Press, Cambridge (1992).

[5] P. Pelcé and A. Pumir, J. Cryst. Growth **73**, 337 (1986).

[6] D. Kessler, J. Koplik, and H. Levine, Phys. Rev. A **34**, 4980 (1986).

[7] E. A. Brener, M. B. Gejlikman, and D. E. Temkin, Zh. Éksp. Teor. Fiz. **94**, 241 (1988).

[8] E. Brener, H. Müller-Krumbhaar, Y. Saito, and D. Temkin, Phys. Rev. E **47**, 1151 (1993).

[9] R. Kupferman, D. A. Kessler, and E. Ben-Jacob, Physica A **231**, 451 (1995).

[10] T. Ihle and H. Müller-Krumbhaar, Phys. Rev. Lett. **70**, 3083 (1993); Phys. Rev. E **49**, 2972 (1994).

[11] E. A. Brener, Yu. Saito, H. Müller-Krumbhaar, D. E. Temkin, Pis'ma Zh. Éksp. Teor. Fiz. **61**, 285 (1995).

[12] M. Ben Amar and E. Brener, Phys. Rev. Lett. **75**, 561 (1995).

[13] J. A. Warren and J. S. Langer, Phys. Rev. A **42**, 3518 (1990); Phys. Rev. E **47**, 2702 (1993).

[14] T. Dombre and V. Hakim, Phys. Rev. A **36**, 2811 (1987).

[15] A. Karma and P. Pelcé, Phys. Rev. A **39**, 4162 (1989).

[16] J. D. Weeks, W. van Saarloos, and M. Grant, J. Cryst. Growth **112**, 244 (1991).

[17] G. P. Ivantsov, Dokl. Akad. Nauk SSSR **58**, 567 (1947).

[18] E. Ben-Jacob, N. Goldenfeld, J. S. Langer, and G. Schön, Phys. Rev. A **29**, 330 (1984).

[19] D. Temkin, J. C. Geminard, and P. Oswald, J. de Phys. (France) **4**, 403 (1994).

[20] E. Brener, H. Müller-Krumbhaar, and D. Temkin, Europhys. Lett. **17**, 535 (1992).

Translation was provided by the Russian Editorial office.